# Near field thermal memory based on radiative phase bistability of VO$_2$

**S A Dyakov**[1], **J Dai**[1], **M Yan**[1] **and M Qiu**[1,2]

[1] Department of Materials and Nano Physics, School of Information and Communication Technology,
KTH Royal Institute of Technology, Electrum 229, 16440 Kista, Sweden
[2] State Key Laboratory of Modern Optical Instrumentation, Department of Optical Engineering, Zhejiang
University, 310027, Hangzhou, People's Republic of China

E-mail: sedyakov@kth.se and minqiu@zju.edu.cn

## Abstract

We report the concept of a near-field memory device based on the radiative bistability effect
in the system of two closely separated parallel plates of SiO$_2$ and VO$_2$ which exchange heat
by thermal radiation in vacuum. We demonstrate that the VO$_2$ plate, having metal-insulator
transition at 340 K, has two thermodynamical steady-states. One can switch between the states
using an external laser impulse. We show that due to near-field photon tunneling between the
plates, the switching time is found to be only 5 ms which is several orders lower than in case
of far field.

Keywords: heat transfer, bistability, memory effect, metal insulator transition, thermal
radiation

(Some figures may appear in colour only in the online journal)

## 1. Introduction

In the past decade, the proposals of thermal analogs of electronic components of integrated circuits, such as transistor [1], diode [2], memory element [3] and logic element [4], attract attention of researchers due to their potential in controlling the heat flow by phonon heat flux for information processing. However the feasibility of this technology is limited by several fundamental constraints [5]. The two main constraints are the speed of heat carriers and the Kapitza resistance also known as interfacial thermal resistance due to the small overlapping of phonon states at the interface of different elements. Another problem in taming the phonons for information processing is that a strong phonon–phonon interaction could result in non-linearity of thermal behavior of the phononic devices. Finally, the stability of the system might be reduced because of radiative losses and thermal fluctuations [6]. On the other hand, the use of photons as heat exchange carriers for spatially isolated objects is free from the aforementioned difficulties that opens new horizons in controlling the heat flow. The radiation-mediated thermal counterparts of diode [7, 8], transistor [5] and self-oscillatory system [9] have been proposed.

Another interesting phenomenon in the systems of radiatively heat exchanging objects is a radiative bistability which was first mentioned by Zhu *et al* in [10] in terms of negative differential thermal conductance for SiC plates. Recently, the concepts of thermal [6] and thermo-mechanical [11] memory devices based on the radiative bistability were introduced. In [6] the memory effect in the system of two parallel SiO$_2$ and VO$_2$ plates originates from the first-order phase transition of VO$_2$ at $T_{ph} = 340$ K [12]. The memory switching characteristics in that work are limited by the far field radiative heat exchange between plates which implies the contribution only of propagating waves. At the same time, when the separation distance between the plates is small enough compared to dominant thermal emission wavelength, the evanescent waves come into play [13]. This leads to sufficient increase of the heat transfer coefficient; from the thermal memory viewpoint, this fact means shortening of the switching time between the stationary states. In this work we focus on the purely radiative bistability effect for the system of VO$_2$ and SiO$_2$ plates in the near field case when the separation distance between the plates is small enough for photon tunneling.
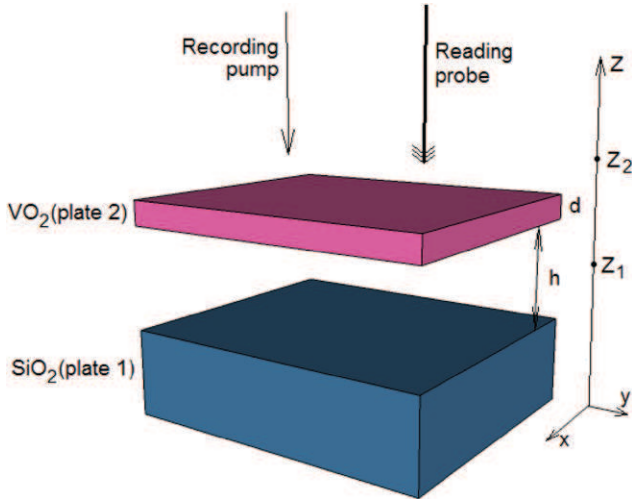
J. Phys. D: Appl. Phys. **48** (2015) 305104

S A Dyakov *et al*



**Figure 1.** The concept of near field thermal memory device consisting of a $SiO_2$ plate and a $VO_2$ plate separated by thin vacuum gap. The system has two stationary states which differ in temperature and phase state of $VO_2$ plate. The external impulse switches between states of $VO_2$ plate.

## 2. Model structure

The concept of the near field thermal memory is shown in figure 1. The structure consists of a semi-infinite $SiO_2$ plate and a thin $VO_2$ plate separated by a vacuum gap. The choice of $SiO_2$ as a material of the first plate is attributed to a strong phonon–phonon coupling between the $SiO_2$ and $VO_2$ insulator inside the vacuum gap [14]. The system is immersed in a thermal bath at temperature of $T_{bath} = 300$ K. The temperature of $SiO_2$ plate is fixed also at 300 K, while the temperature of $VO_2$ is varied. We will show that although the temperature of $SiO_2$ plate is fixed, the system has two thermal stationary states which differ by the phase state of $VO_2$ plate. In the proposed memory device, one-bit data is encoded by one of two stationary states. We will also show that due to the radiative heat exchange between plates, one can use the external laser pulse to switch between these states (see figure 1).

## 3. Theoretical approach

The radiative heat exchange between plates is treated with a formalism of fluctuational electrodynamics [15]. The energy flux of thermal radiation of $i$-th plate at temperature $T_i$ in $z_j$ coordinate is expressed as [16]:

$$F_{ij}(T_i) = \sum_{s,p} \int_0^\infty \frac{d\omega}{2\pi} \Theta(\omega, T_i) \int_0^\infty \frac{k_x dk_x}{2\pi} f_{ij}(\omega, k_x). \quad (1)$$

In the above equation, index $i = 1$ or 2 denotes $SiO_2$ and $VO_2$ plates correspondingly; $z_1$ denotes any coordinate in the separation gap and $z_2$ denotes any coordinate in the upper semi-infinite vacuum; $\omega$ is the angular frequency and $k_x$ is the $x$-component of wavevector; $f_{ij}(\omega, k_x)$ is the monochromatic transmittance of thermal radiation at certain $k_x$; $\Theta(\omega, T_i) = \hbar\omega/[\exp(\hbar\omega/k_B T_i)]$ is the mean energy of Planck oscillator and $k_B$ is Boltzmann's constant. The summation

symbol in expression (1) denotes the accounting for *s*- and *p*-polarizations. The monochromatic transmittance of thermal radiation $f_{ij}(\omega, k_x)$ is calculated in terms of the complex amplitude reflectance and transmittance of the plates. For $k_x < \omega/c$, the coefficients $f_{ij}(\omega, k_x)$ are given by the following expressions:

$$f_{11} = (1-|r_1|^2)(1-|r_2|^2)|D|^{-2}, \quad (2)$$

$$f_{21} = (1-|r_1|^2)(1-|r_2|^2-|t_2|^2)|D|^{-2}, \quad (3)$$

$$f_{12} = (1-|r_1|^2)|t_2|^2|D|^{-2}, \quad (4)$$

$$f_{22} = 1-|r_{02}|^2-(1-|r_1|^2)|t_2|^2|D|^{-2}, \quad (5)$$

where $D = 1 - r_1 r_2 e^{2ik_{z0}h}$ is the Fabry–Perot like denominator and $h$ is the separation distance between plates. For $k_x > \omega/c$

$$f_{11} = f_{21} = 4\text{Im}(r_1)\text{Im}(r_2)e^{-2|k_{z0}|h}|D|^{-2} \quad (6)$$

$$f_{12} = f_{22} = 0. \quad (7)$$

In expressions (2)–(7), $r_i$ and $t_i$ are the complex amplitude reflectance and transmittance of the $i$-th plate, $r_{02}$ is the complex amplitude reflectance of the whole structure from the side of semi-infinite vacuum and $k_{z0}$ is the $z$-component of the wavevector in vacuum. Parameters $r_i$ and $t_i$ can be calculated by means of the scattering matrix method [13, 17, 18]. The Fresnel coefficients that are used in construction of the scattering matrices, accounting for anisotropy of $VO_2$ plate, are described in [7, 19]. Expressions (2), (3) and (6) coincide with those for the transmission coefficients of radiative heat transfer between two semi-infinite plates (see for example [20]) with exception of the part $1-|r_2|^2-|t_2|^2$ in (3) which accounts for the emissivity of $VO_2$ plate [19]. Expressions (4) and (5) can be obtained from the Kirchoff's law by calculating the absorptivities of $VO_2$ and $SiO_2$ plates when the electromagnetic wave irradiates the structure from the semi-infinite vacuum. The corresponding scattering matrix manipulations are quite straightforward and not presented here.

## 4. Results and discussions

At stationary state, the net energy flux emitted or received by $VO_2$ plate vanishes. This is described by the following equation[3]:

$$F_{net}(T_2) \equiv F_{int}(T_2) + F_{bath} + F_{ext} = 0, \quad (8)$$

where $F_{int}(T_2) = F_{11} - F_{12} - F_{21} - F_{22}$ is the power of the heat transfer from $SiO_2$ plate to $VO_2$ plate due to the difference in their temperatures. The term $F_{bath}$ denotes the power which is absorbed in the $VO_2$ plate due to thermal bath and can be calculated as $-F_{int}(T_{bath})$. The term $F_{ext}$ stands for the power which is absorbed in the $VO_2$ plate due to some external energy source. In practice, the external energy source can be either a thermal object, a laser, or an electric heater. In this paper, in order to control the value of $F_{net}$ we take the external energy source as

---

[3] Please note, that $F_{net}$ and $F_{int}$ depend on both $T_1$ and $T_2$.
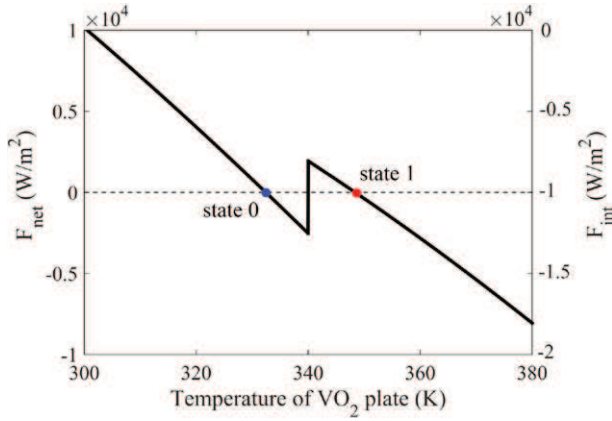
**Figure 2.** The power of the heat transfer from $SiO_2$ plate to $VO_2$ plate due to the difference in their temperatures, $F_{int}(T_2)$, and the net power flux $F_{net}(T_2)$ of $VO_2$ plate as a function of the temperature of $VO_2$ plate. The graph illustrates the negative differential thermal conductance. $h = 50$ nm, $d = 50$ nm, $F_0 = 1.9 \times 10^4$ W m$^{-2}$, $T_{SiO_2} = 300$ K.

a laser beam of 442 nm wavelength, which hits the $VO_2$ plate from the upper semi-infinite vacuum at normal angle of incidence. The wavelength of 442 nm corresponds to equal extinction coefficients of $VO_2$ in amorphous and metallic phases. The power which is absorbed in $VO_2$ plate is $F_{ext} = aF_0$, where $F_0$ is the laser power and $a$ is the absorption coefficient which is calculated by a standard scattering matrix formalism. For $d = 50$ nm, $h = 50$ nm $a \approx 0.53$ for both states of $VO_2$ plate.

At the fixed temperature of $SiO_2$ plate, the zero of the function $F_{net}(T_2)$ defines the steady-state temperature of $VO_2$ plate. In case of absence of the phase transitions, and when the temperature dependence of dielectric constants $\tilde{\varepsilon}_i$ is weak, the function $F_{net}(T_2)$ has a single zero. This situation is described for two parallel SiC plates in [13]. The multiple zeros of the function $F_{net}(T_2)$ may arise due to the essential temperature dependence of dielectric constants of the material that was studied in [10].

Due to the phase transition, the dielectric function $\tilde{\varepsilon}_2$ of $VO_2$ plate has a jump at the phase transition temperature, $T_{ph}$ [14, 21]. This causes the discontinuity of the first kind of the function $F_{net}(T_2)$ at $T_2 = T_{ph}$ that results in the negative differential thermal conductance between two plates (see figure 2). The value of the laser power $F_0 = 1.9 \times 10^4$ W m$^{-2}$ is chosen in such a way that the discontinuity of the function $F_{net}(T_2)$ is located near zero (see right axis scale in figure 2). The function $F_{net}(T_2)$ was calculated for separation distance between plates $h = 50$ nm, thickness of $VO_2$ plate $d = 50$ nm and temperature of $SiO_2$ plate $T_{SiO_2} = 300$ K. The choice of the parameter $d$ is attributed to the wishes to minimize the heat capacitance of $VO_2$ plate in order to accelerate the thermal relaxation. For precisely that reason, the separation distance in turn has to be small enough to ensure efficient near-field photon tunneling from one plate to the other. In this case, the characteristic heat exchange power is of several orders of magnitude higher than in case of the far field, that at a given heat capacitance of $VO_2$ plate yields in sufficient shortening of the thermal relaxation time [13]. On the other hand, the parameters $d$ and $h$ must not be too small from the practical point of view. Thus, the $VO_2$
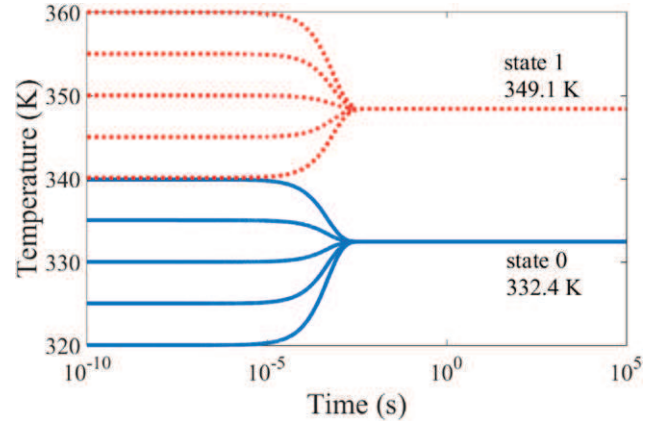


**Figure 3.** The time evolutions of temperature of $VO_2$ plate at various initial values. Solid and dashed lines denote crystalline and metallic phases of $VO_2$ plate correspondingly.

plate has two stationary states which differ by the temperature and the phase state. We call the situation when the $T_2 = 332.4$ K as 'state 0' and $T_2 = 349.1$ K as 'state 1'.

In order to check whether the states 0 and 1 are stable over time let us simulate the temporal dynamics of the $VO_2$ plate temperature. The energy balance equation of the radiative heat transfer dynamics is written as [13, 22]

$$\rho c_v d \frac{dT_2(t)}{dt} = F_{11} - F_{12} - F_{21}(T_2) - F_{22}(T_2) + F_{bath} + F_{ext}(t), \tag{9}$$

with $F_{ext}(t) = aF_0 = $ const. In equation (9), $\rho = 4.6$ g cm$^{-3}$ is the mass density of $VO_2$, $c_v$ is the mass heat capacitance at constant volume of $VO_2$. In calculations, the temperature dependence of the mass heat capacitance of $VO_2$ is accounted for by the Debye model with Debye temperature of 750 K, the molar mass of $85.92$ g mol$^{-1}$ and the number of atoms in $VO_2$ molecule of 3. In equation (9) the spatial temperature distribution inside the plates is assumed to be homogeneous. As it follows from the definition of energy flux $F_{ij}$, equation (9) includes the contributions of radiative heat exchange and thermal emission to the far field. It is worth noting that the dynamical processes such as phase transition stabilization and temperature relaxation inside the plates due to phonons or electrons are neglected in our model since they occur at nanosecond timescale [13, 23].

The solution of integro-differential equation (9) is shown in figure 3 for the initial temperatures of $VO_2$ plate, $T_2(0)$, varied from 320 K to 360 K. In fact, figure 3 demonstrates the bistability in the studied system. Indeed, when the initial temperature of the $VO_2$ plate is less than 340 K, the steady-state temperature is 332.4 K. On the other hand, for $T_2(0) > 340$ K, the steady-state temperature is 349.1 K. These temperatures correspond to those obtained from the analysis of temperature dependence of the net power flux for $VO_2$ plate (see figure 2). In both cases, the phase state of the $VO_2$ plate does not change during the thermalization process. The time it takes for $VO_2$ plate to reach stationary state is 3 ms and is determined by the thickness of $VO_2$ plate, separation distance and the material characteristics [13].

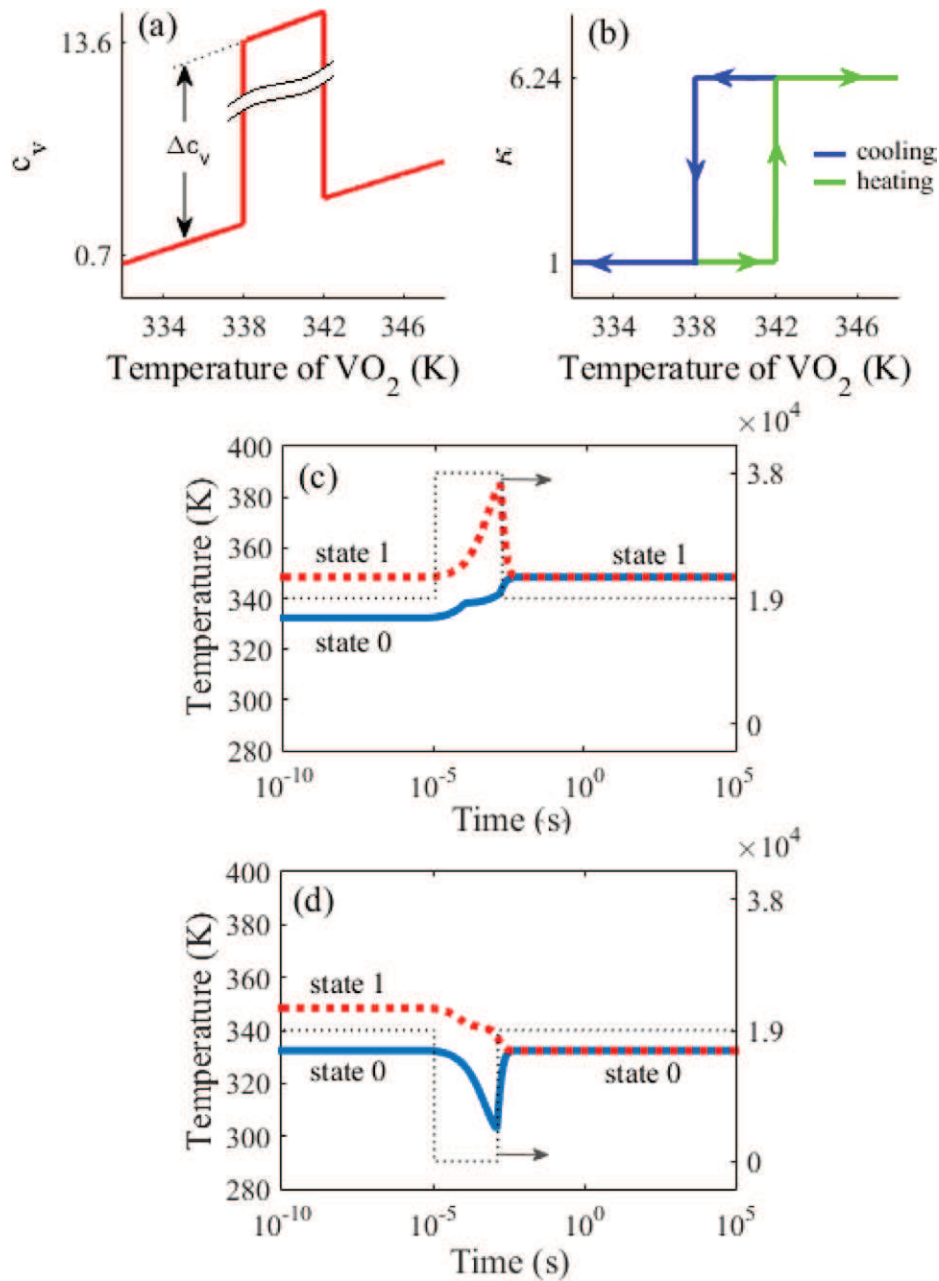J. Phys. D: Appl. Phys. **48** (2015) 305104

S A Dyakov *et al*



**Figure 4.** (a) Temperature dependence of the mass heat capacitance. (b) Imaginary part of refractive index of $VO_2$ at $\omega = 150$ THz near the phase transition temperature. The dynamics of switching of $VO_2$ plate from (c) state 0 to state 1 and (d) from state 1 to state 0. Dotted lines show the switching impulse of external source.

So far, the time evolutions are obtained within assumption that the incident power $F_0$ is constant. When $F_0$ is no longer constant in time, the temperature of $VO_2$ plate is time-dependent. Of particular interest in manipulating of $VO_2$ plate temperature is the case when the function $F_0(t)$ is a single pulse. Let us consider the single rectangular pulse of the external power $F_0(t)$ with the duration of $\Delta t$ and the amplitude of $\Delta F$. Under the action of external pulse, the change of $VO_2$ plate temperature is accompanied by the phase transitions. The metal-insulator transition of $VO_2$ is characterized by the latent heat and hysteresis of the optical constants. In simulation of the time evolutions of $VO_2$ temperature under the external pulse, the latent heat of the phase transition, $L$, is accounted for by assuming that the heat capacitance of $VO_2$ in

the temperature range $\{T_{ph} - \Delta T, T_{ph} + \Delta T\}$ is $c_v = c_{vo} + \Delta c_v$ (see figure 4(a)) [24]. Here $c_{vo}$ is the heat capacitance of $VO_2$ calculated by the Debye model, and the extra heat capacitance $\Delta c_v$ is chosen in such a way that $2\Delta c_v \Delta T = L$, where $\Delta T = 2$ K and $L = 51.49$ J g$^{-1}$ [24]. The hysteresis of optical constants is also accounted for, which is illustrated in figure 4(b) for the extinction coefficient $\kappa$ at $\omega = 150$ THz. We consider that in heating/cooling regime, the optical constants of the $VO_2$ plate remain unchanged until the full amount of latent heat is absorbed. The time evolutions of $VO_2$ temperature under the positive and negative external pulses with amplitudes $\Delta F = \pm 1.9 \times 10^4$ W m$^{-2}$ and durations $\Delta t = 1.7$ and 1.3 ms are shown in figures 4(c) and (d) for two initial temperatures which correspond to states 0 and 1. Note that the negative

J. Phys. D: Appl. Phys. **48** (2015) 305104

S A Dyakov *et al*

amplitude of the external pulse corresponds to decrease of the initial laser power $F_0$ to a value $F_0 - |\Delta F|$. It can be seen from figures 4(a) and (b) that regardless of the initial temperature of $VO_2$ plate, the system thermalizes to state 1 after the action of a positive external pulse and to state 0 after the action of a negative external pulse. The overall time it takes to switch from state 0 to state 1 is 5 ms and from state 1 to state 0 is 4 ms. The pulse durations $\Delta t = 1.7$ and 1.3 ms correspond to the minimal power absorbed in $VO_2$ plate which can result in switching between stationary states. Thus, the time evolutions shown in figures 4(c) and (d) illustrate the switching procedure between states 0 and 1. Therefore, the described impulses of external power can be used for data writing to the thermal memory.

From practical point of view, the separation distance of 50 nm might be too small to be demonstrated. Increase of the separation distance would lead to the less efficient photon tunneling via the near field channels and as a consequence, lower transmittances of thermal radiation $f_{11}$ and $f_{21}$. This causes an increase of the switching time which, in turn, depends not only on the absolute values of fluxes $F_{ij}$, $F_{bath}$ and $F_{ext}$ but also on their relative contributions to the energy balance of $VO_2$ plate. In the light of this, further investigation is needed to describe the influence of geometry, including the effect of boundaries, on the radiative bistability. In what follows we will compare the switching times in the near- and far-field regimes. In order to do that we simulated the switching dynamics for the structure, the same as we considered so far, but with the separation distance of 5 $\mu$m. The resulted switching time is found to be $\sim 10$ s. In the far field, the terms $F_{ij}$ as well as the appropriate value of external power, $F_{ext}$, in equation (9) are three orders of magnitude lower than in the near field [13]. At a given latent heat of the phase transition and thickness of $VO_2$ plate, this yields in longer switching times. The drastic change in characteristic heat exchange rates due to the near field was also reported in [13, 25, 26].

Finally, the information stored in the thermal memory can be read by measurements of transmission or reflection spectra. Our scattering matrix simulations showed that the transmission coefficient of the entire structure at $\lambda = 1450$ nm for the normal incidence of the probe beam (see figure 1) equals to 0.43 in case of crystalline phase of $VO_2$ plate and to 0.23 in case of metallic phase.

## 5. Conclusion

In conclusion, we have theoretically demonstrated the thermal radiative bistability and the memory effect in the system of two parallel plates of $SiO_2$ and $VO_2$ separated by a thin vacuum gap. In this geometry, due to contactless near-field interaction between the plates, the driving heat exchange flux provides 5 ms switching time which more than 3 orders of magnitude faster than in the far field. In spite of the fact that 5 ms switching time is fairly slow, we believe that the discussed structure is a great example of radiative heat flux control by near field that could be useful for practical applications in information processing.

## References

[1] Li B, Wang L and Casati G 2006 Negative differential thermal resistance and thermal transistor *Appl. Phys. Lett.* **88** 143501

[2] Li B, Wang L and Casati G 2004 Thermal diode: rectification of heat flux *Phys. Rev. Lett.* **93** 184301

[3] Wang L and Li B 2008 Thermal memory: a storage of phononic information *Phys. Rev. Lett.* **101** 267203

[4] Wang L and Li B 2007 Thermal logic gates: computation with phonons *Phys. Rev. Lett.* **99** 177208

[5] Ben-Abdallah P and Biehs S-A 2014 Near-field thermal transistor *Phys. Rev. Lett.* **112** 044301

[6] Kubytskyi V, Biehs S-A and Ben-Abdallah P 2014 Radiative bistability and thermal memory *Phys. Rev. Lett.* **113** 074301

[7] Ben-Abdallah P and Biehs S-A 2013 Phase-change radiative thermal diode *Appl. Phys. Lett.* **103** 191907

[8] Otey C R, Lau W T and Fan S 2010 Thermal rectification through vacuum *Phys. Rev. Lett* **104** 154301

[9] Dyakov S A, Dai J, Yan M and Qiu M 2015 Thermal self-oscillations in radiative heat exchange *Appl. Phys. Lett.* **106** 064103

[10] Zhu L, Otey C R and Fan S 2012 Negative differential thermal conductance through vacuum *Appl. Phys. Lett.* **100** 044104

[11] Elzouka M and Ndao S 2014 Near-field nanothermomechanical memory *Appl. Phys. Lett.* **105** 243510

[12] Qazilbash M M *et al* 2007 Mott transition in $vo_2$ revealed by infrared spectroscopy and nano-imaging *Science* **318** 1750–3

[13] Dyakov S A, Dai J, Yan M and Qiu M 2014 Thermal radiation dynamics in two parallel plates: the role of near field *Phys. Rev.* **90** 045414

[14] Yang Y, Basu S and Wang L 2013 Radiation-based near-field thermal rectification with phase transition materials *Appl. Phys. Lett.* **103** 163101

[15] Rytov S M 1959 Theory of electric fluctuations and thermal radiation *Technical Report* DTIC Document

[16] Messina R and Antezza M 2011 Scattering-matrix approach to casimir-lifshitz force and heat transfer out of thermal equilibrium between arbitrary bodies *Phys. Rev.* **84** 042102

[17] Ko D Y K and Inkson J 1988 Matrix method for tunneling in heterostructures: resonant tunneling in multilayer systems *Phys. Rev.* **38** 9945

[18] Francoeur M, Pinar M and Vaillon R 2009 Solution of near-field thermal radiation in one-dimensional layered media using dyadic Green's functions and the scattering matrix method *J. Quant. Spectrosc. Radiat. Transfer* **110** 2002–18

[19] Guo Y and Jacob Z 2014 Fluctuational electrodynamics of hyperbolic metamaterials *J. Appl. Phys.* **115** 234306

[20] Francoeur M, Basu S and Petersen S J 2011 Electric and magnetic surface polariton mediated near-field radiative heat transfer between metamaterials made of silicon carbide particles *Opt. Express* **19** 18774–88

J. Phys. D: Appl. Phys. **48** (2015) 305104

S A Dyakov *et al*

[21] Barker A S, Verleur H W and Guggenheim H J 1966 Infrared optical properties of vanadium dioxide above and below the transition temperature *Phys. Rev. Lett.* **17** 1286–9

[22] Nikbakht M 2015 Three-body radiation dynamics in systems with anisotropic nanoparticles preprint arXiv:1501.04487

[23] Rini M, Cavalleri A, Schoenlein R W, López R, Feldman L C, Haglund R F Jr, Boatner L A and Haynes T E 2005 Photoinduced phase transition in vo2 nanocrystals: ultrafast control of surface-plasmon resonance *Opt. lett.* **30** 558–60

[24] Berglund C N and Guggenheim H J 1969 Electronic properties of VO$_2$ near the semiconductor-metal transition *Phys. Rev.* **185** 1022

[25] Tschikin M, Biehs S-A, Rosa F and Ben-Abdallah P 2012 Radiative cooling of nanoparticles close to a surface *Eur. Phys. J.* **85** 233–40

[26] Messina R, Tschikin M, Biehs S-A and Ben-Abdallah P 2013 Fluctuation-electrodynamic theory and dynamics of heat transfer in systems of multiple dipoles *Phys. Rev.* **88** 104307